I&EC research
Industrial & Engineering Chemistry Research

Article

Cite This: Ind. Eng. Chem. Res. 2018, 57, 11154−11166

pubs.acs.org/IECR

CO_2 Capture in Chemically and Thermally Modified Activated Carbons Using Breakthrough Measurements: Experimental and Modeling Study

Mohsen Karimi,[*,†,‡,§] José A. C. Silva,[*,‡,§] Carmem N. d. P. Gonçalves,[‡] Jose L. Diaz de Tuesta,[†,§] Alírio E. Rodrigues,[†] and Helder T. Gomes[†,§]

[†]Laboratory of Separation and Reaction Engineering - Laboratory of Catalysis and Materials (LSRE/LCM), Department of Chemical Engineering, Faculty of Engineering, University of Porto, Rua Dr. Roberto Frias, S/N, 4099-002 Porto, Portugal

[‡]Laboratory of Separation and Reaction Engineering (LSRE), Department of Chemical and Biological Technology, Polytechnic Institute of Bragança, Campus de Santa Apolonia, 5300-857 Bragança, Portugal

[§]Grupo de Processos e Produtos Sustentáveis, Centro de Investigação de Montanha (CIMO), Instituto Politécnico de Bragança, 5300-253 Bragança, Portugal

Supporting Information

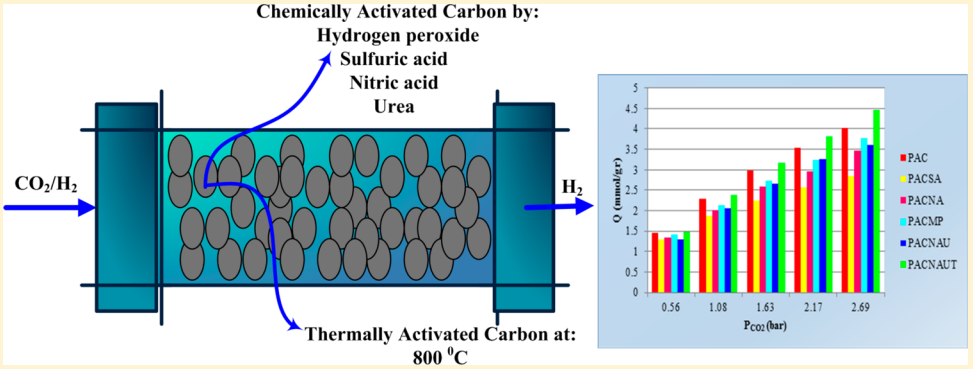

ABSTRACT: The development of adsorption-based technologies for CO_2 capture in the postcombustion processes requires finding materials with high capacity of adsorption and low cost of preparation. In this study, the modification of a commercial activated carbon (Norit ROX 0.8), considered as a solid adsorbent for CO_2 capture, and the effects of different methods of activations, chemically (hydrogen peroxide, sulfuric acid, nitric acid, and urea) and thermally (at 800 °C) on adsorption performance, have been investigated. Then, CO_2 adsorption capacity was studied at different temperatures and pressures to evaluate the effects of various agents on sample performance. The textural properties of the samples were determined using adsorption−desorption isotherms of nitrogen at −196 °C. Finally, the obtained data were modeled by Response Surface Methodology (RSM) and Langmuir isotherm. The results showed that the prepared sample by successive treatments with nitric acid, urea, and thermal calcination has a higher uptake capacity than other modified samples.

1. INTRODUCTION

1.1. Global Warming and CO_2 Capture. Climate change has become one of the primary issues nowadays, which has attracted much attention, observation, and investigation to find a solution for one of the most important environmental challenges and energy policies in the 21st century.[1,2] One of the predominant greenhouse gases is carbon dioxide (CO_2) which its sharp increase in the atmosphere as well as its dangerous effects on the ecosystem contribute to much environmental anxiety for researchers. Tangang et al.[3] declared that the climate changes will cause the enhancement of the surface temperature of earth to around 3−5 °C by the end of this century, which contributes to the ice and glacier melting and rising sea level up to 95 cm.[4] Based on reports,[5] combustion of coal, oil, and natural gas industries, including naphtha refineries[6] and petrochemical complexes,[7] is the source of more than 80% of CO_2 emissions throughout the world; whereas iron, steel, and cement manufacturing are in the next levels.[8] As a consequence of these industrial activities, the CO_2 concentration has had 70 ppm enhancement in the atmosphere from the preindustrial period until now (from 280 to 400 ppm, respectively), while its maximum value should not exceed more than 350 ppm.[9] One of the main strategies to decrease the amount of CO_2 in the atmosphere is Carbon Capture and Storage (CCS),[10] which is able to reduce, control,

Received: March 3, 2018
Revised: June 27, 2018
Accepted: July 19, 2018
Published: July 19, 2018

DOI: 10.1021/acs.iecr.8b00953
Ind. Eng. Chem. Res. 2018, 57, 11154−11166

and optimize the overall mitigation costs by enhancing a great reduction in the greenhouse gas (GHG) emissions.[11,12] CCS is a group of technologies that have the ability to reduce the emission of CO_2 from fixed industrial sources to the atmosphere; which based on the BLUE Map Scenario of the International Energy Agency (IEA), this route can lead to 19% reduction of CO_2 emission (as the most costly component of the CCS process), by 2050.[13] The simple schematic of CCS has been presented in Figure 1.

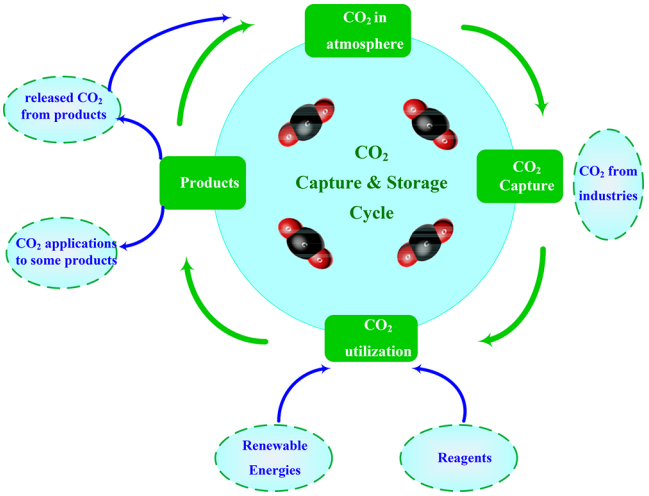

Figure 1. Schematic diagram of carbon dioxide capture and storage (CCS) cycle.

1.2. Physical Adsorption. Currently, chemical adsorption with amine-based sorbents is the most popular technology for CO_2 capture in the postcombustion processes throughout the world. In this method, the flue gas passes through an absorber tower and CO_2 reacts with the amine solution, and then this aqueous solution is transported to the absorber tower, whereby CO_2 is separated at a higher temperature (>100 °C).[14,15] Despite its high performance, this method has several drawbacks, including the following: equipment corrosion and high energy consumption (for the solvent cost and regeneration), as well as the production of a wide range of hazardous substances.[16,17] For these reasons, other strategies, mainly the physical adsorption with porous solid materials, have received much attention in the past years, as an effective and versatile technique for the removal of different classes of pollutants from gaseous or liquid streams.

Various physical adsorbents, such as porous carbons,[18−21] metal organic framework materials,[22−25] zeolite molecular sieves,[26,27] lithium zirconate,[28] silicon based mesoporous materials,[29−31] and other metal oxides materials,[32] have been developed for the CO_2 capture in the recent years. Among these adsorbents, activated carbons are highly attractive for CO_2 adsorption for several reasons. First, these materials are an amorphous porous form of carbon that can be prepared several ways. Agricultural residues, animal wastes, coals, and liquid fractions obtained from the thermal treatments of plant wastes are among the main sources of activated carbon. Also, pyrolysis of different carbon-containing resins, fly ash, and biomass are other ones.[33−36] Thus, cost-effective and abundant resources are two of the main benefits of this adsorbent, whereas synthesis and development of MOFs is one of the main drawbacks of these materials. In addition, hydrophobic character of activated carbons is their main quality when compared to zeolites and MOFs, which reduces the effect of moisture (as an existing component in postcombustion processes) on the adsorption performance.[37] Furthermore, less energy is required for regeneration in the desorption process,[39] due to the weaker physical interaction of activated carbons with CO_2 molecules and having a lower heat of adsorption than zeolites (13X).[38] Thus, these qualities have made activated carbons the promising adsorbent for CO_2 capture.

1.3. Objective. In this work, based on the scope of CCS strategy, the modified activated carbons have been prepared and characterized in our lab (LSRE-LCM). Then, by considering the main challenges of postcombustion carbon capture processes, it has been tested at five different pressures (1, 2, 3, 4, and 5 bar) and three temperatures (40, 70, and 100 °C) using the breakthrough technique. In addition, the results are modeled with Langmuir isotherm and a second-order equation employed from the response surface methodology (RSM). Finally, the obtained values are compared with literature reports to evaluate the reliability of the proposed materials.

2. MATERIAL AND METHODS

2.1. Materials and Chemicals. PAC is an extruded carbon material produced by steam activation. In this study, the commercial powder activated carbon Norit ROX 0.8 with high purity (by having only 3 wt % of ash content) was supplied in cylindrical pellets (diameter and average length were 0.8 and 4.0 mm, respectively). Urea (65 wt %), nitric acid (65 wt %), and sulfuric acid (96−98 wt %) were supplied by Riedel-de-Haën; also hydrogen peroxide (30%, w/v) was obtained from Panreac. In addition, the employed gases, carbon dioxide and helium with purity of 99.98% and 99. 95%, were supplied by Air Liquide.

2.2. Activation Techniques. Thermal and chemical methods are two main techniques for activating carbon based materials. In the thermal activation, the materials are carbonized in the temperature range of 400−850 °C, while in the chemical method by using some chemical agents, activation takes place by heating the mixture of precursors and dehydrating the agent or oxidant.[40] The activated carbon (Norit ROX 0.8) was ground and sieved to particle sizes, ranging from 0.106 to 0.250 mm (PAC material), and then was chemically modified by liquid phase, thermal, and hydrothermal treatments. In this way, three samples were prepared by treating 25 g of PAC with 500 mL of 30% (w/v) H_2O_2 (PACHP sample), 18 M of H_2SO_4 (PACSA sample), and 5 M of HNO_3 (PACNA sample) at room temperature (24 h), 150 °C (3 h), and 110 °C (3 h), respectively. After these treatments, all samples were filtered and washed several times with distillate water until the neutrality of the ringing water. Later, samples were dried at 110 °C in an oven, for 18 h, resulting in PACHP, PACSA, and PACNA materials. Two other samples were obtained in the successive treatments of the PACNA material. The first one was prepared through the treatment of PACNA with 1 M of urea solution (50 mL per 2 g of PACNA) at 200 °C for 2 h, under its own vapor pressure, in a stainless steel high pressure batch reactor. Later, the material was filtered, washed, and dried at the same conditions, resulting in PACNAU material. The last material was obtained from a gas phase thermal treatment of 1 g of the PACNAU sample under N_2 flow (100 $cm^3 \cdot min^{-1}$) at 120, 400, and 600 °C for 1 h at each temperature and then at 800 °C for 4 h, resulting in PACNAUT material.

DOI: 10.1021/acs.iecr.8b00953
Ind. Eng. Chem. Res. 2018, 57, 11154−11166

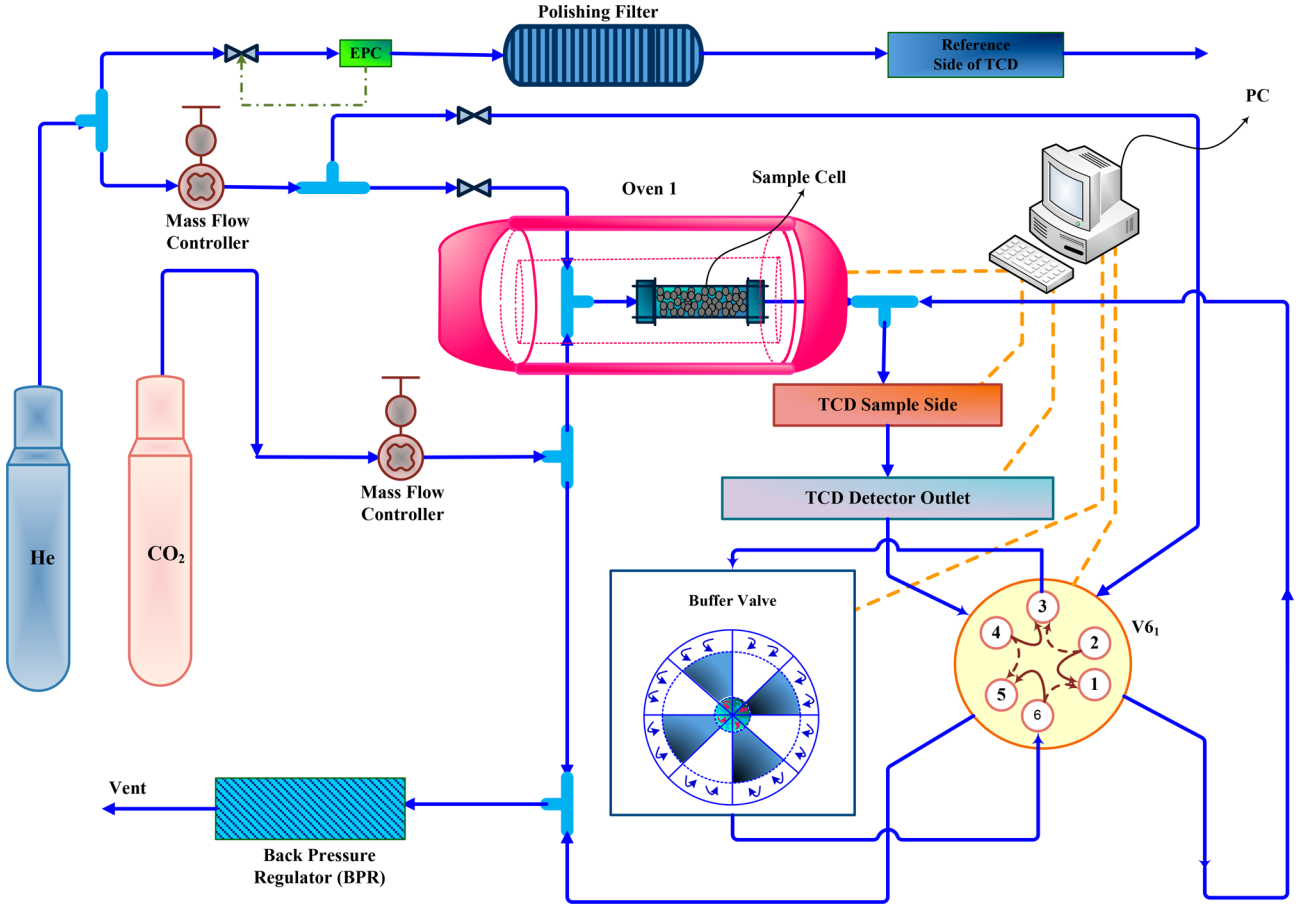

Figure 2. Experimental setup used to measure adsorption equilibrium in modified activated carbons.

2.3. Characterization of Activated Carbons. Textural characterizations of the activated carbons were obtained from N_2 adsorption−desorption isotherms at −196 °C, using a Quanta-chrome NOVA 4200e adsorption analyzer. The BET method[41] was employed to determine the specific surface area (S_{BET}) of activated carbons, and the *t*-method was employed (employing ASTM standard D-6556-01 for the thickness calculation) to determine the external surface area (S_{ext}) and the micropore volume (V_{microp}).[42] Subtracting the S_{ext} from S_{BET} measured the microporous surface area (S_{microp}); also the average pore diameter (D_{microp}) was calculated by approximation ($D_{microp} = 4\ V_{microp}/S_{microp}$). The total pore volume (V_{Total}) was determined at $p/p^0 = 0.98$. In addition, microporosity was evaluated by employing the empiric micropore analysis method of Mikhail et al.[43] (MP) and the theoretical Horvath−Kawazoe (HK) method;[44] also mesoporosity was assessed by using the Barrett−Joyner−Halenda (BJH) method, applied for N_2 adsorption and desorption ($p/p^0 > 0.35$).[45] Calculations of all methods (MP, HK, and BJH) were performed by employing NovaWin software v11.02. Elemental compositions (C, H, N, and S) were quantified by applying a Carlo Erba EA 1108 Elemental Analyzer.

2.4. Breakthrough Technique. In this study, the CO_2 adsorption/desorption experiments were accomplished by a breakthrough technique using the homemade apparatus at LSRE-LCM (the experimental apparatus was made with stainless steel tubing, Swagelok Company, USA), which has its schematic shown in Figure 2. A detailed description of this unit was presented in an author's previous study.[23]

Briefly, the experimental procedure has three main steps: the first one is preparation, the second one consists of adsorption runs, and the last one is the analysis of the obtained data. At the first step, an adsorption column, which has been made up from the stainless steel, was packed with one of the activated carbons. Then, the preparation of the samples was performed by passing a hot carrier gas (helium) for 12 h in the column. After that, a constant flow rate of the mixture (carrier gas and CO_2) which is done by a three-way valve ($V3_1$ flow goes from a to b) is sent to the system. In this process, CO_2 flow rate is controlled by a mass flow controller (MFC). An electronic pressure controller (EPC) is used for He flow rate measurement. Then, the adsorption process takes place at the selected partial pressure and temperature by passing the gas mixture through the fixed bed (which has been put in the oven). In this work, five different adsorption pressures were tested at three different temperatures for each material. To analyze the performance of the process during the adsorption runs, a thermal conductivity detector (TCD) continuously measured the mass flow at the output of the packed bed as a time function (breakthrough curve). This measurement is continued until the output composition reaches the value of inlet gas composition in the bed, which is the saturation condition.

The collected data by the computer are in the voltage signals, and they are converted to the flow rate as a time function. Then, by applying a mass balance on the bed, the equilibrium loading is obtained for a specific temperature and partial pressure of CO_2, as follows:

DOI: 10.1021/acs.iecr.8b00953
Ind. Eng. Chem. Res. 2018, 57, 11154−11166

$$Q_{CO_2} = \frac{1}{m_{adsorbent}}\left[\int_0^{t_s}(F_{CO_2,in} - F_{CO_2,out})dt - \frac{y_{CO_2,feed}P_b\varepsilon_T V_b}{ZR_gT_b} - \frac{y_{CO_2,feed}P_b V_d}{ZR_gT_b}\right] \quad (1)$$

In this equation, t_s is the saturation time of the bed, and ε_T is the total porosity of the bed, which is calculated by the following relation[46]

$$\varepsilon_T = \varepsilon_b + (1 - \varepsilon_b)\varepsilon_p \quad (2)$$

where ε_p is the particle porosity, and ε_b is the packed bed porosity. The definition of all the other variables has been presented in the nomenclature section. Finally, in a similar cycle, the desorption process takes place by switching the gas flow rate to the carrier gas to desorb the adsorbed CO_2 on the bed. In Figure 3, the adsorption/desorption cycle has been

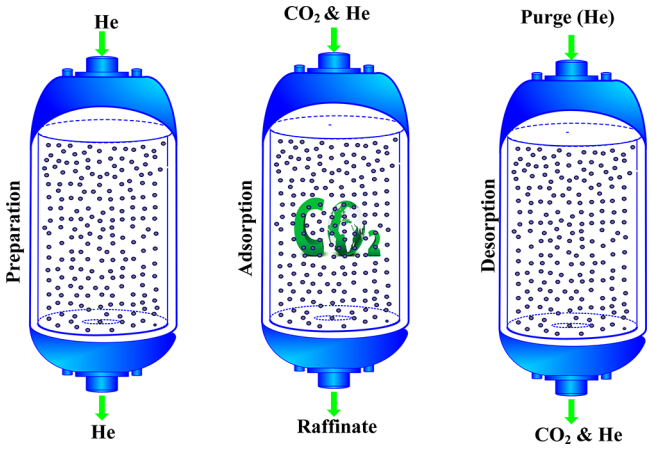

Figure 3. Configuration of the adsorption−desorption cycle of CO_2 capture.

depicted for more clarification. Furthermore, the characteristics of adsorption unit and operating conditions of these experiments are reported in Table 1.

3. MODELING AND SIMULATION

3.1. Langmuir Model (Isotherm Study). In order to investigate the behavior of the adsorption process, the analysis of the adsorption equilibrium data is required. In this way, using theoretical models is one of the best strategies to study the experimental equilibrium isotherms. Among the various available adsorption models, the Langmuir model is the best one to describe the chemisorption reaction, due to the restriction to the monolayer formation.[47,48] Thus, the Langmuir model has been selected to investigate and correlate the equilibrium results in this study. The basic assumptions in this model are each site can only hold one adsorbate molecule, the adsorption energy of all sites is the same, there are definite adsorption sites, and there is no interaction between adsorbed molecules on the neighboring sites.[48] The mathematical formula of the Langmuir model is as follows

$$Q_e = \frac{Q_m K_L P_{CO_2}}{1 + K_L P_{CO_2}} \quad (3)$$

where Q_e is the adsorption capacity at equilibrium condition, Q_m is the maximum adsorption capacity, P_{CO_2} is the partial pressure of CO_2, and K_L is the Langmuir adsorption constant, related to the free energy of the adsorption and it is a criteria to measure how strong an adsorbate molecule is attached to the site, which can be adjusted from the following relation

$$K_L = \frac{\alpha \exp(\Delta H/R_gT)}{k_{d\infty}\sqrt{2\pi M R_g T}} = K_\infty \exp(\Delta H/R_gT) \quad (4)$$

$$K_\infty = \frac{\alpha}{k_{d\infty}\sqrt{2\pi M R_g T}} \quad (5)$$

where ΔH is the heat of adsorption, α is the sticking coefficient, T is the temperature, and M is the molecular weight. The validity of the obtained model is evaluated by the coefficient of determination (R^2), which its scale is [0−1], and for the best fitting it should be close to the unit.

3.2. Response Surface Methodology (RSM). In this study, after performing the breakthrough measurements to determine the uptake capacities of prepared samples for CO_2 capture, RSM methodology was employed for the statistical analysis of the adsorption process. The selected runs for the considered samples are based on the full factorial design with two factors (temperature and partial pressure of CO_2), which have 3 (40, 70, and 100 °C) and 5 (1, 2, 3, 4, and 5 bar) levels. Since the runs are enough to obtain the second-order equation, typically it is used in the RSM (more experiments than coefficients). Also, it is possible to employ the methodology in order to study the variance of the response variable with the factors or independent variables. In this sense, the analysis of the obtained experimental values as well as the interaction effects of parameters has been evaluated by using the Historical

Table 1. Specific Properties and Operating Conditions of Breakthrough Apparatus

Bed Characteristics						
parameter	value					
bed inner diameter (cm)	0.46					
bed length (cm)	10					
wall thickness (cm)	0.089					
Total Parameters of Experiments						
	PAC	PACSA	PACHP	PACNA	PACNAU	PACNAUT
mass of sample (g)	∼0.6	∼0.6	∼0.6	∼0.6	∼0.6	∼0.6
ambient pressure (bar)	1	1	1	1	1	1
ambient temperature (K)	293.75	295.55	294.85	295.25	293.05	294.35
CO_2 flow rate (mL/min)	∼10	∼10	∼10	∼10	∼10	∼10
helium flow rate (mL/min)	∼9	∼9	∼9	∼9	∼9	∼9
particle sizes (μm)	106−250	106−250	106−250	106−250	106−250	106−250
porosity (total volume porous, $mm^3 \cdot g^{-1}$)	541	520	545	547	581	635

DOI: 10.1021/acs.iecr.8b00953
Ind. Eng. Chem. Res. 2018, 57, 11154−11166

Data tool of the Design Experts software v.8.0. The CO_2 uptake capacity (Q) and the breakthrough time (t_b) are the outputs of the adsorption process which are considered as response variables, whereas the CO_2 partial pressure (P_{CO_2}) and the temperature (T) are supposed to be the independent variables. Then, the response variables are modeled by fitting the following polynomial function:

$$y = \beta_0 + \beta_1 x_1 + \beta_2 x_2 + \beta_{12} x_1 x_2 + \beta_{11} x_1^2 + \beta_{22} x_2^2 + \varepsilon \quad (6)$$

In this relation, y is the response variable (Q or t_b); x_1 and x_2 are the independent variables (P_{CO_2} and T), which take the coded values from −1 to 1, proportionally and accordingly with the minimal and maximum values of the selected operating conditions (e.g., x_2 takes the values of −1, −0.5, 0, 0.5, and 1 for the partial pressure of 0.56, 1.09, 1.62, 2.16, and 2.68 bar). β_0 is an intercept coefficient, β_1 and β_2 express the linear coefficients, β_{12} is a coefficient to display the interaction between operating parameters, β_{11} and β_{22} express the quadratic coefficients of operating conditions, and the last term (ε) is a residual error.[39] The fit of the equations and determination of coefficient values were realized by using the Design Expert v8.0 software. The statistical evaluation of the model to evaluate the fitness of the quadratic model to the experimental data was employed by the analysis of variance (ANOVA) and the lack-of-fit, which tested the significance of the regression model and the individual model coefficients.[49] Both of them were performed also with the software. The probability of the coefficients (p-value) was employed to detect whether a model and its coefficients are significant or not. Finally, by using the adjusted coefficient of determination (Adj-R^2) the accuracy of the model is checked.[50]

Table 2. Elemental Analysis of the Proposed Activated Carbons for CO_2 Adsorption

	C (%)	H (%)	S (%)	N (%)	remaining (%)	PZC
PAC	79.0	1.5	0.6	0.0	18.9	7.6
PACSA	76.1	1.8	1.2	0.0	20.9	5.8
PACHP	81.4	1.4	0.6	0.0	16.5	6.8
PACNA	70.6	2.4	0.4	1.4	25.2	2.0
PACNAU	75.3	2.7	0.3	3.2	18.4	6.1
PACNAUT	88.6	2.2	0.4	2.8	5.9	10.3

4. RESULTS AND DISCUSSION

4.1. Characterizations of Adsorbents. The elemental analysis, related to the C, H, S, and N content of the prepared activated carbons, is summarized in Table 2. As can be seen, the carbon and hydrogen content was lightly modified, whereas sulfur and nitrogen concentrations were increased by modifying the original activated carbon. As expected, the S-content was increased from 0.6% (PAC) to 1.2% (PACSA) with the sulfuric acid treatment. The nitrogen percentage was also enhanced with nitric acid and urea treatments to reach 1.4% and 3.2% for PACNA and PACNAU samples (commercial carbon does not have nitrogen), respectively. However, the N-content of the PACNAUT sample was lower than PACNAU, likely due to the thermal process, which produces the desorption of nitrogen superficial groups with weak bonds. The remaining analysis (the content that is not C, H, S, or N), which is typically assumed to be ash and oxygen, was significantly low for this sample. Probably, the desorption of weak oxygen superficial groups also takes place during the thermal treatment of the sample. Furthermore, the significant increase of the C-content of PACNAUT was observed because of thermal treatment.[51]

Nitrogen adsorption−desorption isotherms of the prepared adsorbents have been presented in Figure 4. As can be observed, adsorbents exhibit a mixed type of I and IV isotherms,[52] to which more uptake capacity at low p/p^0 corresponds with the filling of micropores. Furthermore, hysteresis loop presence of the isotherms can be classified as H4 type, based on the last classification of IUPAC, that is typically found for micro-mesoporous carbon materials.[52,53] On the other hand, based on the textural properties which were determined from the N_2 sorption analysis (summarized in Table 3), samples are more near to the microporous category (V_{mic}/V_{Total} higher than 0.5) than mesoporous, with an average width of micropores (W_{mic}) of ca. 1.72 nm. For more information, the t-plots of the adsorbents have been depicted in Figure S1 (Supporting Information).

The pore size distribution of the adsorbents was assessed by BJH, HK, and MP methods, as shown in Figure 5. Based on

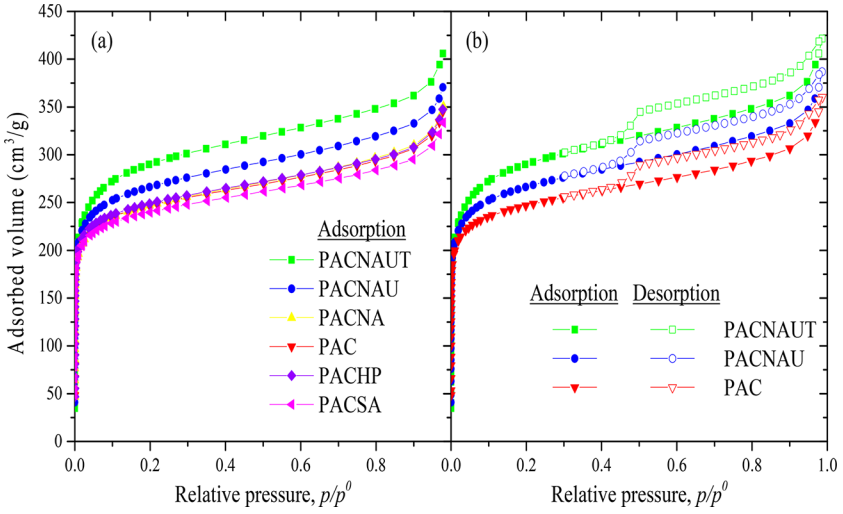

Figure 4. Isotherms of nitrogen (a) adsorption of all the studied powdered activated carbon samples and (b) adsorption−desorption of selected samples.

DOI: 10.1021/acs.iecr.8b00953
Ind. Eng. Chem. Res. 2018, 57, 11154−11166

Table 3. Textural Properties of the Proposed Activated Carbons Determined from BET and t-Plot Methods

	S_{BET} (m^2/g)	S_{ext} (m^2/g)	S_{mic} (m^2/g)	V_{mic} (mm^3/g)	V_{mic}/V_{Total} (%)	W_{mic} (nm)
PAC	885 ± 10	160 ± 2	725 ± 12	314 ± 1	58	1.73 ± 0.03
PACSA	862 ± 9	150 ± 2	712 ± 11	308 ± 1	59	1.72 ± 0.03
PACHP	893 ± 10	159 ± 2	734 ± 12	319 ± 1	58	1.73 ± 0.03
PACNA	889 ± 10	170 ± 2	719 ± 12	311 ± 1	57	1.72 ± 0.03
PACNAU	960 ± 11	181 ± 2	778 ± 12	336 ± 1	58	1.72 ± 0.03
PACNAUT	1055 ± 11	197 ± 2	858 ± 12	367 ± 1	58	1.71 ± 0.03

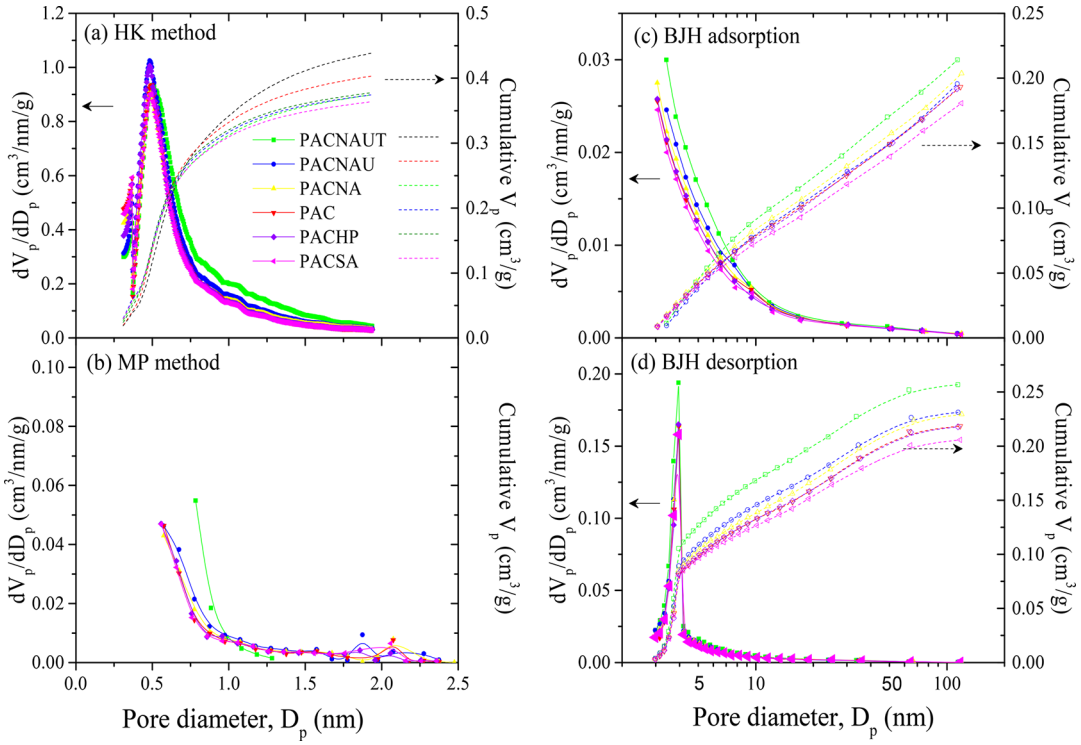

Figure 5. Pore distribution in the powdered activated carbons from N_2 adsorption−desorption analysis and determined by (a) HK and (b) MP methods for microporous range and the BJH method in (c) adsorption and (d) desorption of N_2 for mesoporous assessment.

the BJH method, it is observed that the pore size range is kept below 5.0 nm for all materials, with a pronounced fraction of micropores which was found when HK and MP methods are used.

According to the textural properties (Table 3), there is a slight increase in S_{BET} values which results from a proportional increase in the formation of micropores, which contributes to the fairly similar V_{mic}/V_{Total} values and average micropore diameters (W_{mic}). For instance, the S_{BET} in PACNAUT increases 19.2% when compared to PAC, due to the increment of the micropore volume, 16.9% (from 314 to 367 cm^3/g). Despite the increased values of S_{BET} and V_{mic}, the surface chemistry is more affected by the applied treatments. For instance, when PAC is treated with nitric acid (PACNA), the amount of oxygen-containing groups (mainly carboxylic acids) is substantially increased (as inferred by the remaining 25.2 wt % in the elemental analysis, attributed to the ash and oxygen, Table 2), and an acidic material has been obtained, as assessed by the determination of Point of Zero Charge values of the materials (as been mentioned in Table 2). In addition, further treatment of PACNA with urea (PACNAU) contributes to the incorporation of nitrogen-containing groups at the surface of the materials. As shown in Table 2, the increase of the N content at the expense of oxygen content produces a less acidic material. Finally, thermal treatment of PACNAU under inert atmosphere (obtained PACNAUT) leads to the decomposition of carboxylic acids, resulting in less O content materials (with lower remaining wt %) and more pronounced basic character. In conclusion, despite the significant role of the porosity on the adsorption, the surface chemistry of the materials is also considerable.

4.2. CO_2 Adsorption. The high adsorption capacity is one of the key parameters of an ideal adsorbent for CO_2 capture, and it can be contributed to the reduction of the volume of the sorbent requirement, decreasing the sorbent bed, apparatus size, and finally capital costs.[54] The analysis of adsorption isotherms is one of the best strategies to evaluate the adsorbent performance in adsorption−desorption cyclic processes. To this goal, the obtained adsorption isotherms of prepared carbon materials are reported in Figure 6(a-f). As can be observed, the adsorption capacities of all prepared samples are enhanced by increasing P_{CO_2}, based on P_{CO_2} the thermodynamic driving force of the adsorption process. On the other hand, as expected, the increment of the temperature has a negative impact on the uptake capacity of adsorbents, in an accommodation with the exothermicity behavior of the adsorption process. In this way, the increase of temperature, which corresponds with the enhancement of energy of molecules, results in an increment of

DOI: 10.1021/acs.iecr.8b00953
Ind. Eng. Chem. Res. 2018, 57, 11154−11166

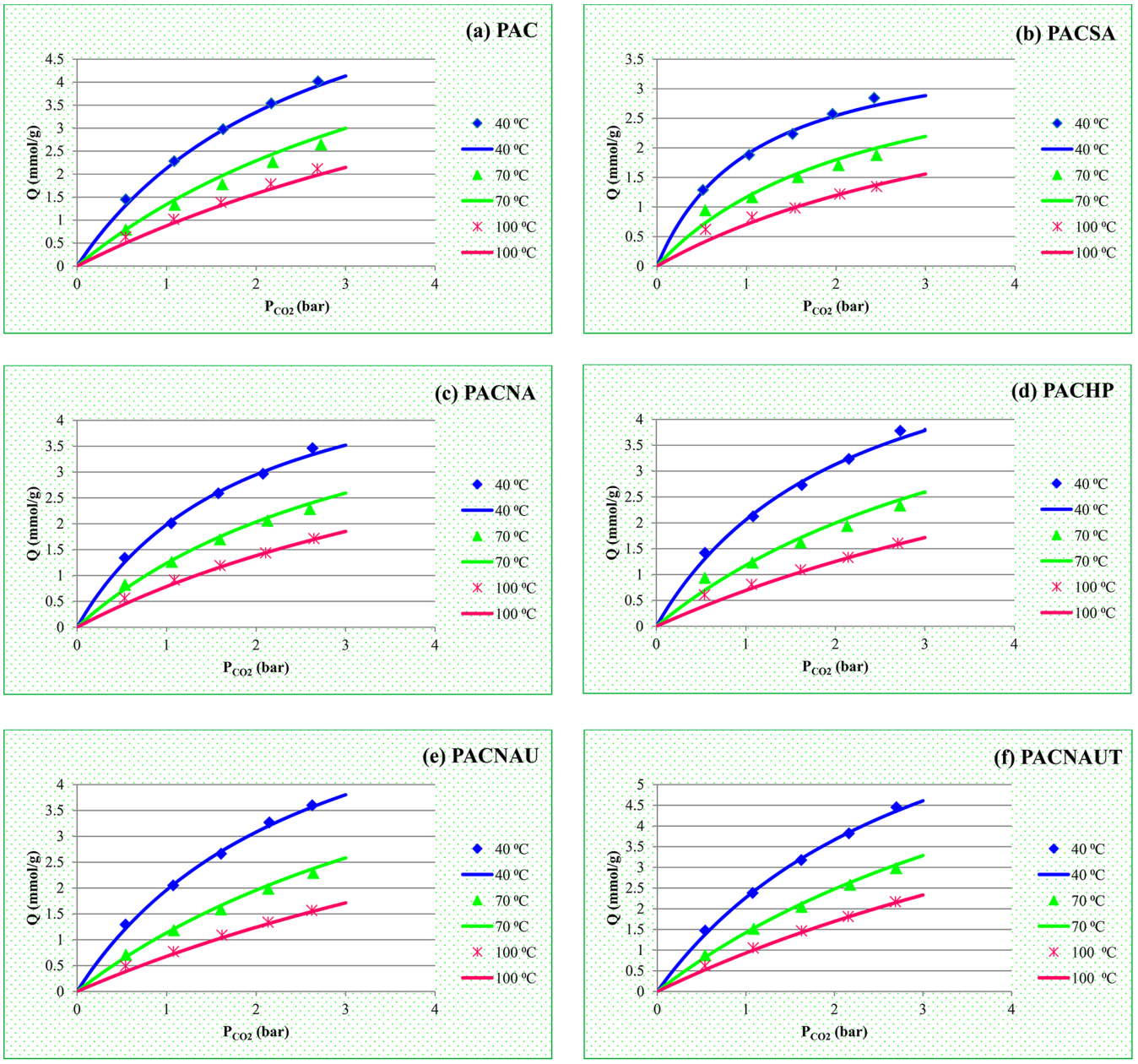

Figure 6. Experimental equilibrium (symbols) data and fitted Langmuir isotherm (lines) for CO_2 adsorption at 40, 70, and 100 °C with (a) PAC, (b) PACSA, (c) PACNA, (d) PACHP, (e) PACNAU, and (f) PACNAUT materials.

the diffusion rate of gaseous molecules, but at the same time, it decreases the possibility of capturing or trapping CO_2 molecules on the adsorbent surface by fixed energy adsorption sites.[55−57] In fact, the increase of temperature provides the sufficient energy for the adsorbed gases to overcome the van der Waals attraction forces employed by the sorbent surface and migrate back to the gas phase.[55] On the other hand, the higher surface adsorption energy and molecular diffusion at the enhanced temperatures contribute to the instability of the adsorbed CO_2 molecules on the carbon surface, and this results in the acceleration of the desorption process.[58]

The experimental data of adsorption process were illustrated by the Langmuir model. In Figure 6(a-f), marker points represent the experimental data, whereas the solid curves express the results of the applied isotherm model. As can be observed, the Langmuir model is well-fitted with the behavior of the experimental adsorption results. The Langmuir parameters and the determination coefficient (R^2) are reported in Table 4.

A comparison between the uptake capacities of sorbents for CO_2 capture in the various temperatures and partial pressures is depicted in Figure 7(a, b, c) (the numerical values for better grasp have been reported in Table S1, Supporting Information). As can be seen, in all plots, by increasing the pressure of adsorption, the uptake capacities of the samples increase; also the temperature enhancement has had a negative impact on the adsorption capacity. This behavior is the same for all the considered samples. Regarding the uptake capacity of the materials, PACSA, which has been treated with sulfuric acid, shows the worst performance, and PACNAUT, that has been chemically (with nitric acid and urea) and thermally treated, is the best one. The higher performance of PACNAUT can be interpreted by considering several factors. First, based on the

DOI: 10.1021/acs.iecr.8b00953
Ind. Eng. Chem. Res. 2018, 57, 11154−11166

Table 4. Langmuir Parameters at Different Temperatures Using Linearized Technique

		samples					
T (°C)	Langmuir coefficients	PAC	PACHP	PACSA	PACNA	PACNAU	PACNAUT
40	Q_m	17.57	21.93	23.29	19.43	20.73	17.19
	K_L	0.373	0.462	0.926	0.527	0.378	0.314
	R^2	0.9778	0.9697	0.9474	0.9665	0.9787	0.9821
70	Q_m	17.57	21.93	23.29	19.43	20.73	17.19
	K_L	0.207	0.221	0.423	0.274	0.188	0.176
	R^2	0.9899	0.9886	0.9784	0.9865	0.9919	0.9923
100	Q_m	17.57	21.93	23.29	19.43	20.73	17.19
	K_L	0.126	0.119	0.219	0.159	0.105	0.108
	R^2	0.9956	0.9959	0.9914	0.9935	0.997	0.9965

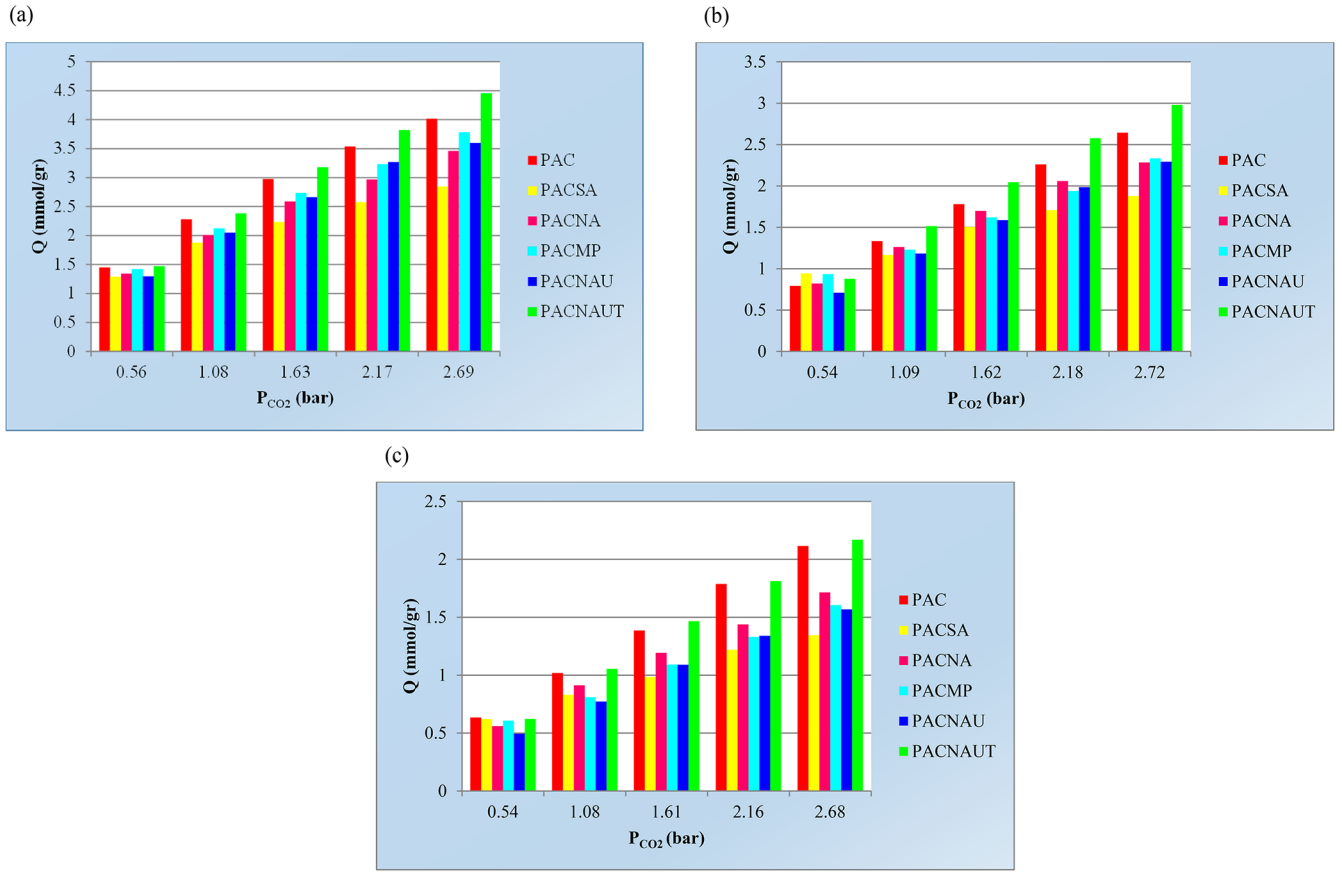

Figure 7. Comparison between CO_2 uptake capacity (mmol/g) of investigated adsorbents at (a) 40 °C, (b) 70 °C, and (c) 100 °C.

textural properties of PACNAUT (reported in Table 3), it has the highest microporous volume and size which contributes to adsorbing a greater amount of CO_2. Also, PACNAUT has increased around 12% C-content of the adsorbent (Table 2), which can be one of the other main evaluators of PACNAUT performance. In addition, the higher adsorption capacity can be also ascribed to the desorption of weak superficial groups as a consequence of the thermal treatment at 800 °C (as previously discussed), leading to the apparition of possible adsorption sites and removal of functional groups able to block some pores. On the other hand, the samples resulting from the chemical treatments by sulfuric acid, nitric acid, and hydrogen peroxide have reduced the point of zero charge (PZC) by boosting the acidity of materials, which contributes to the lower number of the available electrons on the carbon surface, since most of the oxygen-containing functionalities on the surface have an electron withdrawing capacity.[55,59] While by applying the nitrogen-containing functionalities, upon chemical treatment with the urea, it enhances the PZC of PACNU by decreasing the acidity, and consequently the reduction of acidic active sites, and a large increment of the basic active sites (main parameter on the adsorption process). Then, the subsequent thermal treatment of PACNU intensifies the elimination of acidic active sites by thermal decomposition and preparation of a sample by a high percentage of the basic active sites. These results confirm that PACNUT is the sample with the lowest concentration of the oxygen-containing functionalities (as shown in Table 2), which has the highest number of the available electron donating active sites.[55,59−61] For more information, a comparison between some of the recently proposed sorbents for CO_2 adsorption has been presented in Table 5. As can be seen, the adsorption capacity of PACNAUT, which has been presented in this study, is higher than previous ones.

DOI: 10.1021/acs.iecr.8b00953
Ind. Eng. Chem. Res. 2018, 57, 11154−11166

Table 5. Comparison between the Capacities (mmol/g) of Maximum CO_2 Adsorption on Various Adsorbents

adsorbent	type of activation	porosity	P (bar)	temp (K)	adsorption capacity (mmol·g^{-1})	refs
AHEP (algae)	KOH activation	micro/mesoporous	1	298	1.39	62
				323	0.413	
				348	0.211	
A (1) −700 (char derived)	KOH activation	microporous	1	298	3.136	63
				373	0.704	
B (1) −700 (char derived)	KOH activation	microporous	1	298	0.84	63
				373	0.16	
C (1) − 700 (char derived)	KOH activation	microporous	1	298	1.25	63
				373	0.34	
GKOSN800 (Biomass Olive Stones)	CO_2 and heat treatment	micro/mesoporous	1	298	1.954	64
				373	0.59	
P−C (polyethylene terephthalate)	KOH activation	microporous	1	298	1.09	65
				373	0.273	
AC-MEA	MEA activation	micro/mesoporous	1	303	1.559	66
				343	1.132	
				373	0.575	
				393	0.125	
HCM-DAH-1 (carbon monoliths)	amines	meso/macroporous	1	298	0.9295	67
32ACSH3	NaOH activation	microporous	1	308	0.6159	68
AAM-silica	n/a	micro/mesoporous	1	318	0.78	69
				333	0.58	
				348	0.49	
				363	0.43	
CB−FM	magnetic fine particles	micro/mesoporous	1	291	0.38	57
empty fruit bunch AC	KOH activation	microporous	1	298	2.634	70
				323	1.743	
coconut AC	CO_2 activation	microporous	1	298	1.79	71
				323	1.27	
				373	0.43	
Norit SX2 (peat)	steam activation	mesoporous	1	298	1.88	72
				323	1.29	
				373	0.61	
PACNAUT (Modifed Norit ROX 0.8)	nitric acid, urea and thermally (800 °C)	micro/mesoporous	1	313	**1.4721**	this work
				343	**0.8773**	
				373	**0.6220**	

4.3. CO_2 Capture Analysis Using RSM. The methodology of the response surface was applied for the obtained results with the highlighted materials (PACNAUT and PAC) using the Historical Data tool of RSM. It contributed two correlations to estimate the adsorption capacities of sorbents in different operational conditions. The employed data which have been utilized to develop RSM models are specified in Table S1 (Supporting Information). In this way, the multiple regression analysis and the evaluation of the fitness of models by ANOVA were accomplished to determine the lack of fits and the statistical conditions of the system. Then, the initial models were analyzed and tested for p-value, the standard deviation, R^2, the predicted determination coefficient (Pred-R^2), adjusted R^2 (Adj-R^2), and the lack of fit. Lastly, by determining the insignificant parameters and the interactions in the process, the final models were derived with the acceptable accuracies. The results of ANOVA for CO_2 capture capacity ($mmolCO_2/g$) and breakthrough time (t_b) of PACNAUT are reported in Table 6; also the outcomes of PAC are presented in the Supporting Information. As can be observed, both Q and t_b models are statistically significant since p-value <0.0001, and the lack of fits are not significant. On the other hand, the R^2, Adj-R^2, and the standard deviation results have acceptable values, 0.9988, 0.9981, and 0.047 for CO_2 uptake capacity and 0.9895, 0.9836, and 0.19 for breakthrough time, respectively. The final models (coefficients for real values of the operating conditions, instead of coded values) for the process are as follows:

$$Q = 2.146 - 0.048T + 2.128P_{CO_2} - (0.0109T \times P_{CO_2}) + 0.0003T^2 - 0.106{P_{CO_2}}^2 \quad (7)$$

$$t_b = 5.394 - 0.056T + 0.981P_{CO_2} - (0.017 \times T \times P_{CO_2}) + 0.0003T^2 + 0.516P^2 \quad (8)$$

Coded coefficients of the adsorption capacity equation (Table 6) illustrate that the linear coefficients (−0.82 and 1.1 for T and P_{CO_2}, respectively) have more effect on the variable responses, when compared with other effects (<0.35). In addition, the interaction (−0.35) and second-order coefficients (0.25 and −0.12 for T and P_{CO_2}, respectively) are also significant (p-value <0.0001) in the proposed model. The negative value of the linear coefficient of the temperature means that the temperature enhancement contributes to the reduction of the response variable (Q). According to the value of the interaction coefficient, at the high temperature, the pressure increase has less effect on the increment of the CO_2 uptake

DOI: 10.1021/acs.iecr.8b00953
Ind. Eng. Chem. Res. 2018, 57, 11154−11166

Table 6. Results of Multiple Regression Analysis and Analysis of Variance (ANOVA) for the Proposed Polynomial Model to the CO_2 Capture Capacity and Breakthrough Time

	CO_2 capture capacity, Q (mmol/g_{CO_2})						breakthrough time, t_b (min)					
	sum of squares	mean squares	coded coefficient	standard error	df	p-value	sum of square	mean squares	coded coefficient	standard error	df	p-value
model	16.67	3.33			5	<0.0001	31.6	6.32			5	<0.0001
T	6.67	6.67	−0.82	0.015	1	<0.0001	9.95	9.95	−1.00	0.061	1	<0.0001
P_{CO_2}	9.09	9.91	1.1	0.017	1	<0.0001	18.77	18.77	1.58	0.071	1	<0.0001
$T \times P_{CO_2}$	0.62	0.62	−0.35	0.021	1	<0.0001	1.5	1.5	−0.55	0.087	1	0.0001
T^2	0.21	0.21	0.25	0.026	1	<0.0001	0.35	0.35	0.32	0.11	1	0.0134
$P_{CO_2}^2$	0.04	0.04	−0.12	0.029	1	0.0022	0.94	0.94	0.60	0.12	1	0.0007
residual	0.02	0.002			9		0.34	0.037			9	
total	16.69	-			14		31.93				14	
SD	**0.047**						**0.19**					
R^2	**0.9988**						**0.9895**					
Adj-R^2	**0.9981**						**0.9836**					
Pred-R^2	**0.9944**						**0.9667**					

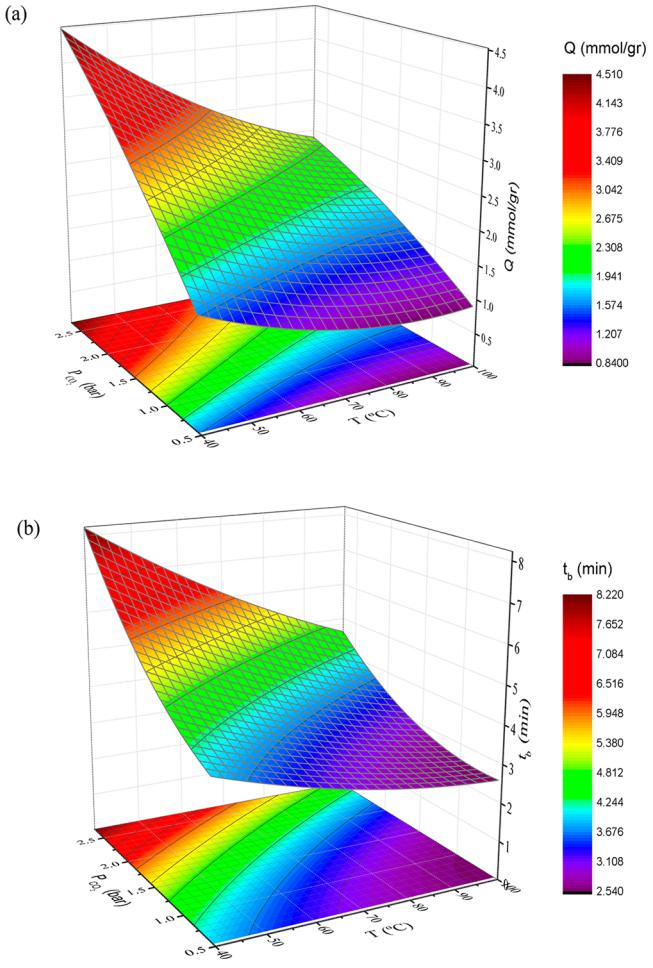

Figure 8. Response surface plots for (a) CO_2 capture capacity (mmol/g) and (b) breakthrough time (t_b), as a function of the independent variables for PACNAUT.

capacity. For example, the adsorption capacity was 1.47 mmol/g and increased up to 4.45 mmol/g at 40 °C, whereas the increment was 1.55 mmol/g at 100 °C (0.62 to 2.16 mmol/g), when the total pressure was raised from 1 to 5 bar.

For more clarification about the behavior of the adsorption process, the three-dimensional response surface plots for the CO_2 capture capacity and the breakthrough time (t_b), as a function of the independent variables, have been depicted in Figure 8. As can be expected, based on Le Chatelier's principle, by increasing the P_{CO_2} and the temperature reduction the CO_2 capture capacity enhances (Figure 8a). Also, with the same behavior (Figure 8b), the P_{CO_2} enhancement and the temperature decrement contribute to increase the breakthrough time (more details about this behavior can be found in the Supporting Information).

5. CONCLUSION

In this study, the potential of hydrogen peroxide, sulfuric acid, nitric acid, and urea as chemical modifiers of commercial activated carbon (Norit ROX 0.8) for CO_2 capture was investigated. In this way, the breakthrough measurements in the fixed bed adsorption column were performed at the temperature (40, 70, and 100 °C) and pressure ranges (1−5 bar) of postcombustion processes. The equilibrium adsorption capacity of the considered samples was evaluated with the Langmuir model as a standard adsorption model, and it showed a satisfactory agreement between the equilibrium data and the modeling results. In addition, isothermic comparison of the prepared samples revealed that the adsorption capacity of PACNAUT, which has been treated by nitric acid and urea followed by the thermal activation at 800 °C under the inert atmosphere, has the highest performance between the prepared materials. Finally, the statistical analysis of the obtained results of PACNAUT and PAC with the Response Surface Methodology (RSM) was performed to evaluate the behavior of the adsorption process and determine the effects and the interactions of the main independent variables (temperature and CO_2 partial pressure) on CO_2 capture capacity and breakthrough time. The results indicated that the partial pressure is the main factor, whose increment increases the CO_2 capture capacity and the breakthrough time.

■ ASSOCIATED CONTENT

Supporting Information

The Supporting Information is available free of charge on the ACS Publications website at DOI: 10.1021/acs.iecr.8b00953.

Appendix A: t-plot of sample adsorbents. Appendix B: breakthrough adsorption measurement. Appendix C: adsorption capacity of the adsorbents. Appendix D: RSM results for CO_2 capture on PAC (PDF)

DOI: 10.1021/acs.iecr.8b00953
Ind. Eng. Chem. Res. 2018, 57, 11154−11166

AUTHOR INFORMATION

Corresponding Authors

*Phone: +351 225081671. E-mail: mohsen.karimi@fe.up.pt (M.K.).

*Phone: +351 273 30 3125. E-mail: jsilva@ipb.pt (J.A.C.S.).

ORCID

Mohsen Karimi: 0000-0002-1886-5454

Alírio E. Rodrigues: 0000-0002-0715-4761

Notes

The authors declare no competing financial interest.

ACKNOWLEDGMENTS

This work was financially supported by Project POCI-01-0145-FEDER-006984 − Associate Laboratory LSRE-LCM funded by FEDER through COMPETE2020 - Programa Operacional Competitividade e Internacionalização (POCI) − and by national funds through FCT - Fundação para a Ciência e a Tecnologia. M.K. also acknowledges a research grant awarded under project "VALORCOMP" (ref.0119_VALORCOMP_2_P), financed through INTERREG V A Spain Portugal (POCTEP) 2014-2020, under the European Regional Development Fund by FCT.

NOMENCLATURE

D_{microp} = average pore diameter (mm)
$F_{CO_{2,in}}$ = molar flow rate of CO_2 at the inlet of bed (mL/min)
$F_{CO_{2,out}}$ = molar flow rate of CO_2 at the outlet of bed (mL/min)
H = hydrogen
K_L = Langmuir adsorption constant (bar $^{-1}$)
K_∞ = affinity constant (bar $^{-1}$)
M = molecular weight (g/mmol)
$m_{adsorbent}$ = mass of adsorbent in the bed (g)
N = nitrogen
O = oxygen
P_b = pressure of bed at equilibrium (bar)
P_{CO_2} = partial pressure of CO_2 (bar)
Q_e = adsorption capacity at equilibrium condition (mmol/g)
Q_m = maximum adsorption capacity (mmol/g)
R^2 = regression coefficient (−)
S = sulfur
S_{BET} = specific surface area (m^2/g)
S_{ext} = external surface area (m^2/g)
S_{microp} = microporous surface area (m^2/g)
t_b = breakthrough time (min)
t_s = saturation time (min)
T_b = temperature of bed at equilibrium (K)
V_b = bed volume (cm^3)
V_d = dead volume (cm^3)
V_{microp} = micropore volume (mm^3/g)
V_{Total} = total pore volume (mm^3)
W_{mic} = width of micropore (nm)
$y_{CO_{2,feed}}$ = molar fraction of CO_2 in feed stream (−)
Z = CO_2 compressibility factor at P_b and T_b (−)

ABBREVIATIONS

PAC = powdered activated carbon
PACHP = powdered activated carbon hydrogen peroxide
PACNA = powdered activated carbon nitric acid
PACNAU = powdered activated carbon nitric acid urea
PACNAUT = powdered activated carbon nitric acid urea thermally
PACSA = powdered activated carbon sulfuric acid

SUBSCRIPTS/SUPERSCRIPTS

Ads = adsorbent
Tot = total
min = minute

GREEK LETTERS

α = sticking coefficient
ε = residual error (−)
ε_b = packed bed porosity (−)
ε_P = particle porosity (−)
ε_T = total porosity of bed (−)
ΔH = heat of adsorption (kJ/mol)

REFERENCES

(1) Karimi, M.; Rahimpour, M. R.; Rafiei, R.; Jafari, M.; Iranshahi, D.; Shariati, A. Reducing environmental problems and increasing saving energy by proposing new configuration for moving bed thermally coupled reactors. *J. Nat. Gas Sci. Eng.* **2014**, *17*, 136−150.

(2) Nurrokhmah, L.; Mezher, T.; Abu-Zahra, M. R. M. Evaluation of handling and reuse approaches for the waste generated from MEA-based CO capture with the consideration of regulations in the UAE. *Environ. Sci. Technol.* **2013**, *47* (23), 13644−13651.

(3) Tangang, F. T.; Liew, J.; Salimun, E.; Kwan, M. S.; Loh, J. L.; Muhamad, H. Climate change and variability over Malaysia: gaps in science and research information. *Sains Malays.* **2012**, *41*, 1355−1366.

(4) Hamdan, M. E.; Man, N.; Yassin, S. M.; D'Silva, J. L.; Shaffril, H. M. Farmers' adaptive capacity towards the impacts of global warming: A review. *Asian Soc. Sci.* **2013**, *9*, 177−184.

(5) Quadrelli, R.; Peterson, S. The energy−climate challenge: Recent trends in CO_2 emissions from fuel combustion. *Energy Policy* **2007**, *35*, 5938−5952.

(6) Karimi, M.; Rahimpour, M. R.; Rafiei, R.; Shariati, A.; Iranshahi, D. Improving thermal efficiency and increasing production rate in the double moving beds thermally coupled reactors by using differential evolution (DE) technique. *Appl. Therm. Eng.* **2016**, *94*, 543−558.

(7) Iranshahi, D.; Karimi, M.; Amiri, S.; Jafari, M.; Rafiei, R.; Rahimpour, M. R. Modeling of naphtha reforming unit applying detailed description of kinetic in continuous catalytic regeneration process. *Chem. Eng. Res. Des.* **2014**, *92*, 1704−1727.

(8) Zhao, C.; Chen, X.; Zhao, C. K_2CO_3/Al_2O_3 for capturing CO_2 in flue gas from power plants. Part 1: carbonation behaviors of K_2CO_3/Al_2O_3. *Energy Fuels* **2012**, *26* (2), 1401−1405.

(9) Wennersten, R.; Sun, Q.; Li, H. The future potential for carbon capture and storage in climate change mitigation - An overview from perspectives of technology, economy and risk. *J. Cleaner Prod.* **2015**, *103*, 724−736.

(10) Sumida, K.; Rogow, D. L.; Mason, J. A.; McDonald, J. M.; Bloch, E. D.; Herm, Z. R.; Bae, T. H.; Long, J. R. Carbon dioxide capture in metal-organic frameworks. *Chem. Rev.* **2012**, *112*, 724−781.

(11) Metz, B.; Davidson, O.; de Coninck, H.; Loos, M.; Meyer, L. *Carbon Dioxide Capture and Storage*; University Press: Cambridge, 2005.

(12) Li, F.; Fan, L. Clean coal conversion processes − progress and challenges. *Energy Environ. Sci.* **2008**, *1*, 248−267.

(13) Figueroa, J.; Fout, T.; Plasynski, S.; McIlvried, H.; Srivastava, R. D. Advances in CO_2 capture technology -The U.S. Department of Energy's Carbon Sequestration Program. *Int. J. Greenhouse Gas Control* **2008**, *2*, 9−20.

(14) Ramdin, M.; de Loos, T. W.; Vlugt, T. J. State-of-the-art of CO_2 capture with ionic liquids. *Ind. Eng. Chem. Res.* **2012**, *51*, 8149−8177.

(15) Wang, Z.; Mitch, W. A. Influence of dissolved metals on N-nitrosamine formation under amine-based CO_2 capture conditions. *Environ. Sci. Technol.* **2015**, *49*, 11974−11981.

(16) McDonald, J. D.; Kracko, D.; Doyle-Eisele, M.; Garner, C. E.; Wegerski, C.; Senft, A.; Knipping, E.; Shaw, S.; Rohr, A. Carbon capture and sequestration: An exploratory inhalation toxicity

DOI: 10.1021/acs.iecr.8b00953
Ind. Eng. Chem. Res. 2018, 57, 11154−11166

assessment of amine -trapping solvents and their degradation products. *Environ. Sci. Technol.* **2014**, *48*, 10821−10828.
(17) Yang, H.; Xu, Z. H.; Fan, M. H.; Gupta, R.; Slimane, R. B.; Bland, A. E.; Wright, I. Progress in carbon dioxide separation and capture: A review. *J. Environ. Sci.* **2008**, *20*, 14−27.
(18) Arenillas, A.; Smith, K. M.; Drage, T. C.; Snape, C. E. CO_2 capture using some fly ash-derived carbon materials. *Fuel* **2005**, *84*, 2204−2210.
(19) Siriwardane, R. V.; Shen, M. S.; Fisher, E. P.; Poston, J. A. Adsorption of CO2 on molecular sieves and activated carbon. *Energy Fuels* **2001**, *15*, 279−284.
(20) Radosz, M.; Hu, X. D.; Krutkramelis, K.; Shen, Y. Q. Flue-gas carbon capture on carbonaceous sorbents: toward a low-cost multifunctional carbon filter for "green" energy producers. *Ind. Eng. Chem. Res.* **2008**, *47*, 3783−3794.
(21) Pevida, C.; Drage, T. C.; Snape, C. E. Silica-templated melamine−formaldehyde resin derived adsorbents for CO2 capture. *Carbon* **2008**, *46*, 1464−1474.
(22) Yazaydın, A. O.; Snurr, R. Q.; Park, T. H.; Koh, K.; Liu, J.; LeVan, M. D.; et al. Screening of metal−organic frameworks for carbon dioxide capture from flue gas using a combined experimental and modeling approach. *J. Am. Chem. Soc.* **2009**, *131* (51), 18198−18199.
(23) Bastin, L.; Barcia, P. S.; Hurtado, E. J.; Silva, J. A. C.; Rodrigues, A. E.; Chen, B. A Microporous Metal-Organic Framework for Separation of CO_2/N_2 and CO_2/CH_4 by Fixed-Bed Adsorption. *J. Phys. Chem. C* **2008**, *112*, 1575−1581.
(24) Millward, A. R.; Yaghi, O. M. Metal−organic frameworks with exceptionally high capacity for storage of carbon dioxide at room temperature. *J. Am. Chem. Soc.* **2005**, *127* (51), 17998−17999.
(25) Bárcia, P. S.; Bastin, L.; Hurtado, E. J.; Silva, J. A. C.; Rodrigues, A. E.; Chen, B. Single and Multicomponent Sorption of CO_2, CH_4 and N_2 in a Microporous Metal-Organic Framework. *Sep. Sci. Technol.* **2008**, *43*, 3494−3521.
(26) Konduru, N.; Lindner, P.; Assaf, A. N. M. Curbing the greenhouse effect by carbon dioxide adsorption with zeolite 13X. *AIChE J.* **2007**, *53*, 3137−3143.
(27) Silva, J. A. C.; Cunha, A. F.; Schumann, K.; Rodrigues, A. E. Binary adsorption of CO_2/CH_4 in binderless beads of 13X zeolite. *Microporous Mesoporous Mater.* **2014**, *187*, 100−107.
(28) Ochoa-Fernández, E.; Ronning, M.; Grande, T.; Chen, D. Nanocrystalline lithium zirconate with improved kinetics for high-temperature CO2 capture. *Chem. Mater.* **2006**, *18* (6), 1383−1385.
(29) Kim, S. N.; Son, W. J.; Choi, J. S. CO_2 adsorption using amine-functionalized mesoporous silica prepared via anionic surfactant-mediated synthesis. *Microporous Mesoporous Mater.* **2008**, *115*, 497−503.
(30) Ma, X. L.; Wang, X. X.; Song, C. S. 'Molecular Basket" Sorbents for separation of CO_2 and H_2S from various gas streams. *J. Am. Chem. Soc.* **2009**, *131* (16), 5777−5783.
(31) Hu, J.; Liu, H. L. CO_2 adsorption on porous materials: experimental and simulation study. *ACS Symp. Ser.* **2010**, *1056*, 209−232.
(32) Yang, Q.; Lin, Y. S. Kinetics of carbon dioxide sorption on perovskite-type metal oxides. *Ind. Eng. Chem. Res.* **2006**, *45*, 6302−6310.
(33) Ioannidou, O.; Zabaniotou, A. Agricultural residues as precursors for activated carbon production−A review. *Renewable Sustainable Energy Rev.* **2007**, *11*, 1966−2005.
(34) Thote, J. A.; Iyer, K. S.; Chatti, R.; Labhsetwar, N. K.; Biniwale, R. B.; Rayalu, S. S. In situ nitrogen enriched carbon for carbon dioxide capture. *Carbon* **2010**, *48*, 396−402.
(35) Balsamo, M.; Budinova, T.; Erto, A.; Lancia, A.; Petrova, B.; Petrov, N.; Tsyntsarski, B. CO_2 adsorption onto synthetic activated carbon: Kinetic, thermodynamic and regeneration studies. *Sep. Purif. Technol.* **2013**, *116*, 214−221.
(36) Choi, S.; Drese, J. H.; Jones, C. W. Adsorbent materials for carbon dioxide capture from large anthropogenic point sources. *ChemSusChem* **2009**, *2*, 796−854.
(37) Plaza, M. G.; García, S.; Rubiera, F.; Pis, J. J.; Pevida, C. Post-combustion CO_2 capture with a commercial activated carbon: Comparison of different regeneration strategies. *Chem. Eng. J.* **2010**, *163*, 41−47.
(38) Silva, J. A. C.; Schumann, K.; Rodrigues, A. E. Sorption and kinetics of CO_2 and CH_4 in binderless beads of 13X zeolite. *Microporous Mesoporous Mater.* **2012**, *158*, 219−228.
(39) Wahby, A.; Ramos-Fernandez, J.; Martinez-Escandell, M.; Sepulveda-Escribano, A.; Silvestre-Albero, J.; Rodriguez-Reinoso, F. High-Surface-Area carbon molecular sieves for selective CO_2 adsorption. *ChemSusChem* **2010**, *3*, 974−981.
(40) Rodriguez-Reinoso, F. Production and applications of activated carbons. In *Handbook of Porous Solids*; Schuth, F., Sing, K. S. W., Weitkarnp, J., Eds.; Wiley-VCH: Weinheim, 2002; pp 1766−1821, DOI: 10.1002/9783527618286.ch24a.
(41) Brunauer, S.; Emmett, P. H.; Teller, E. Desorption of gases in multimolecular layers. *J. Am. Chem. Soc.* **1938**, *60* (2), 309−319.
(42) Lippens, B. C.; de Boer, J. H. Studies on pore systems in catalysts: V. The *t* method. *J. Catal.* **1965**, *4*, 319−323.
(43) Mikhail, R. S.; Brunauer, S.; Bodor, E. E. Investigations of a complete pore structure analysis: I. Analysis of micropores. *J. Colloid Interface Sci.* **1968**, *26*, 45−53.
(44) Horváth, G.; Kawazoe, K. Method for the calculation of effective pore size distribution in molecular sieve carbon. *J. Chem. Eng. Jpn.* **1983**, *16*, 470−475.
(45) Barrett, E. P.; Joyner, L. G.; Halenda, P. P. The determination of pore volume and area distribution in porous substances. I. Computations from nitrogen isotherms. *J. Am. Chem. Soc.* **1951**, *73* (1), 373−380.
(46) Becnel, J. M.; Holland, C. E.; McIntyre, J.; Matthews, M. A.; Ritter, J. A. Fundamentals of fixed bed adsorption processes: analysis of adsorption breakthrough and desorption elution curves. In *American Society for Engineering Education Annual Conference & Exposition*; Montréal, Quebec, Canada, 2002.
(47) Pérez, N.; Sanchez, M.; Rincon, G.; Delgado, L. Study of the behavior of metal adsorption in acid solutions on lignin using a comparison of different adsorption isotherms. *Lat. Am. Appl. Res.* **2007**, *37*, 157−162.
(48) Langmuir, I. The constitution and fundamental properties of solids and liquids. Part I. Solids. *J. Am. Chem. Soc.* **1916**, *38* (11), 2221−2295.
(49) García, S.; Gil, M. V.; Pis, J. J.; Rubiera, F.; Pevida, C. Cyclic operation of a fixed-bed pressure and temperature swing process for CO_2 capture: experimental and statistical analysis. *Int. J. Greenhouse Gas Control* **2013**, *12*, 35−43.
(50) Bas, D.; Boyacı, I. H. Modeling and optimization I: usability of response surface methodology. *J. Food Eng.* **2007**, *78*, 836−845.
(51) Darvishi Cheshmeh Soltani, R.; Safari, M.; Rezaee, A.; Godini, H. Application of a compound containing silica for removing ammonium in aqueous media. *Environ. Prog. Sustainable Energy* **2015**, *34*, 105−111.
(52) Thommes, M.; Kaneko, K.; Neimark, A. V.; Olivier, J. P.; Rodriguez-Reinoso, F.; Rouquerol, J.; Sing, K. S. W. Physisorption of gases, with special reference to the evaluation of surface area and pore size distribution (IUPAC Technical Report). *Pure Appl. Chem.* **2015**, *87*, 1051−1069.
(53) Patrick, J. *Porosity in carbons: characterization and applications*; Halsted Press: New York, 1995.
(54) Bhatta, L. K. G.; Subramanyam, S.; Chengala, M. D.; Olivera, S.; Venkatesh, K. Progress in hydrotalcite like compounds and metal-based oxides for CO_2 capture: a review. *J. Cleaner Prod.* **2015**, *103*, 171−196.
(55) Ribeiro, R. S.; Silva, A. M. T.; Figueiredo, J. L.; Faria, J. L.; Gomes, H. T. The influence of structure and surface chemistry of carbon materials on the decomposition of hydrogen peroxide. *Carbon* **2013**, *62*, 97−108.
(56) Zhou, X.; Yi, H.; Tang, X.; Deng, H.; Liu, H. Thermodynamics for the adsorption of SO_2, NO and CO_2 from flue gas on activated carbon fiber. *Chem. Eng. J.* **2012**, *200−202*, 399−404.

DOI: 10.1021/acs.iecr.8b00953
Ind. Eng. Chem. Res. 2018, 57, 11154−11166

(57) Ammendola, P.; Raganati, F.; Chirone, R. CO_2 adsorption on a fine activated carbon in a sound assisted fluidized bed: Thermodynamics and kinetics. *Chem. Eng. J.* **2017**, *322*, 302−313.
(58) Maroto-Valer, M. M.; Tang, Z.; Zhang, Y. CO_2 capture by activated and impregnated anthracites. *Fuel Process. Technol.* **2005**, *86*, 1487−1502.
(59) Santos, V. P.; Pereira, M. F. R.; Faria, P. C. C.; Órfão, J. J. M. Decolourisation of dye solutions by oxidation with H_2O_2 in the presence of modified activated carbons. *J. Hazard. Mater.* **2009**, *162*, 736−742.
(60) Prabhavathi Devi, B. L. A.; Gangadhar, K. N.; Sai Prasad, P. S.; Jagannadh, B.; Prasad, R. B. N. A glycerol-based carbon catalyst for the preparation of biodiesel. *ChemSusChem* **2009**, *2* (7), 617−620.
(61) Serp, P.; Figueiredo, J. L. *Carbon materials for catalysis*; John Wiley & Sons, Inc.: Hoboken, NJ, 2009.
(62) Zhang, Z.; Wang, K.; Atkinson, J. D.; Yan, X.; Li, X.; Rood, M. J.; Yan, Z. Sustainable and hierarchical porous Enteromorpha prolifera based carbon for CO_2 capture. *J. Hazard. Mater.* **2012**, *229-230*, 183−191.
(63) Olivares-Marin, M.; Garcia, S.; Pevida, C.; Wong, M. S.; Maroto-Valer, M. The influence of the precursor and synthesis method on the CO_2 capture capacity of carpet waste-based sorbents. *J. Environ. Manage.* **2011**, *92*, 2810−2817.
(64) Plaza, M. G.; Pevida, C.; Arias, B.; Fermoso, J.; Casal, M. D.; Martin, C. F.; Rubiera, F.; Pis, J. J. Development of low-cost biomass-based adsorbents for postcombustion CO_2 capture. *Fuel* **2009**, *88*, 2442−2447.
(65) Arenillas, A.; Rubiera, F.; Parra, J. B.; Ania, C. O.; Pis, J. J. Surface modification of low cost carbons for their application in the environmental protection. *Appl. Surf. Sci.* **2005**, *252*, 619−624.
(66) Maroto-Valer, M. M.; Lu, Z.; Zhang, Y.; Tang, Z. Sorbents for CO_2 capture from high carbon fly ashes. *Waste Manage.* **2008**, *28*, 2320−2328.
(67) Hao, G. P.; Li, W. C.; Qian, D.; Wang, G. H.; Zhang, W. P.; Zhang, T.; Wang, A. Q.; Schuth, F.; Bongard, H. J.; Lu, A. H. Structurally designed synthesis of mechanically stable poly (benzoxazine-co-resol) -based porous carbon monoliths and their application as high-performance CO_2 capture sorbents. *J. Am. Chem. Soc.* **2011**, *133* (29), 11378−11388.
(68) Tan, Y. L.; Azharul Islam, M.; Asif, M.; Hameed, B. H. Adsorption of carbon dioxide by sodium hydroxide-modified granular coconut shell activated carbon in a fixed bed. *Energy* **2014**, *77*, 926−931.
(69) Zhao, Y.; Shen, Y.; Bai, L.; Ni, S. Carbon dioxide adsorption on polyacrylamide-impregnated and breakthrough modeling silica gel and breakthrough modeling. *Appl. Surf. Sci.* **2012**, *261*, 708−716.
(70) Parshetti, G. K.; Chowdhury, S.; Balasubramanian, R. Biomass derived low-cost microporous adsorbents for efficient CO_2 capture. *Fuel* **2015**, *148*, 246−254.
(71) Rashidi, N. A.; Yusup, S.; Borhan, A.; Loong, L. H. Experimental and modelling studies of carbon dioxide adsorption by porous biomass derived activated carbon. *Clean Technol. Environ. Policy* **2014**, *16*, 1353−1361.
(72) Rashidi, N. A.; Yusup, S.; Borhan, A. Isotherm and thermodynamic analysis of carbon dioxide on activated carbon. *Procedia Eng.* **2016**, *148*, 630−637.

DOI: 10.1021/acs.iecr.8b00953
Ind. Eng. Chem. Res. 2018, 57, 11154−11166